Supporting Information

Catalyst-free contact-electro-catalytic H_2O_2 synthesis via simple combination of poly(tetrafluoroethylene) stir bar and ultrasound

Authors: Yao Wang,[a] Yanfeng Wang,[*a, b] Baowei Hu,[a] Muqing Qiu,[a] Guandao Gao,[c] Peiyun Wei,[*a, b]

Affiliations:

[a]School of Life and Environmental Sciences, Shaoxing University, Huancheng Road 508, Shaoxing 312000, China.

[b]Department of Environmental Science, Zhejiang University, Yuhangtang Road 866, Hangzhou310058, China.

[c]State Key Laboratory of Pollution Control and Resource Reuse, School of Environment, Nanjing University, Nanjing 210023, China.

*Correspondence to: wangyanfeng@usx.edu.cn; peiyunwei@usx.edu.cn

This PDF file includes:

Figure S1 to S8
Table S1 to S2
Supporting References

Materials and methods

Materials and Reagents

PTFE stir bar and stainless steel stir bar were purchased from Henghua Experimental Co., Ltd. Potassium titanium (IV) oxalate, 5,5-dimethyl-1-pyrolin-N-oxide (DMPO), dimethyl sulfoxide (DMSO), tert-butanol (TBA), were supplied by Macklin. Commercially available H_2O_2 test papers were purchased from Hangzhou Luheng Biotechnology Co., Ltd. Calcium chloride ($CaCl_2$), Calcium nitrate ($Ca(NO_3)_2$), Sodium chloride (NaCl), Magnesium nitrate ($Mg(NO_3)_2$), Magnesium chloride ($MgCl_2$), Aluminum chloride ($AlCl_3$), Zinc chloride ($ZnCl_2$), Sodium sulfate (Na_2SO_4), Sodium carbonate (Na_2CO_3) and Sodium Phosphate (Na_3PO_4) and glucose were purchased from Sinopharm Chemical Reagent Co. Ltd., Shanghai, China.

Experimental Procedure

H_2O_2 production in the PTFE stir bar + ultrasound system. 50 mL deionized water was exposed to ultrasound irradiation (Model JP040S, 240 W, Skymen, China) and continuous mechanical stirring (Model JJ-1, Jintan Co. Ltd, China) in ambient conditions, 1 mL sample solution was taken out every 30 minutes for testing. The pH was adjusted with 1 M of dilute H_2SO_4 or NaOH. Notably, the effect of ultrasonic power on H_2O_2 generation was conducted in an ultrasonic cleaner (Model KQ-250DA, 250 W, Kunshan Shumei, China) with adjustable power.

Quantitative characterization of H_2O_2 Production.

The concentration of H_2O_2 was determined using the potassium titanium (IV) oxalate method. To prepare the potassium titanium (IV) oxalate reagent, a solution was made by dissolving 7.083 g of potassium titanium (IV) oxalate in 136 mL of 98% H_2SO_4 and 114 mL of deionized water. Subsequently, 0.5 mL of the sample and 0.5 mL of potassium titanium (IV) oxalate reagent were combined in a 10 mL colorimetric tube and then diluted to 5 mL. The resulting mixture was analyzed using a UV–vis spectrophotometer (Shimadzu, UV-2600) at a wavelength of 400 nm. The concentration of H_2O_2 was

determined using the equation provided in Figure S8. The high correlation coefficient (R^2 = 0.9997) indicates that the calibration curve is accurate and reliable.

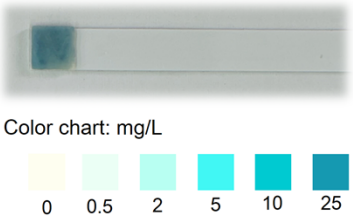

Figure S1. The photo of commercial H_2O_2 test paper exposed to H_2O_2 produced in the PTFE stir bar + ultrasound system.

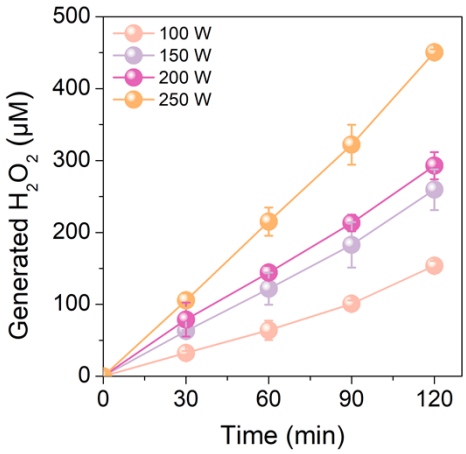

Figure S2. Effect of ultrasonic power on H_2O_2 generation.

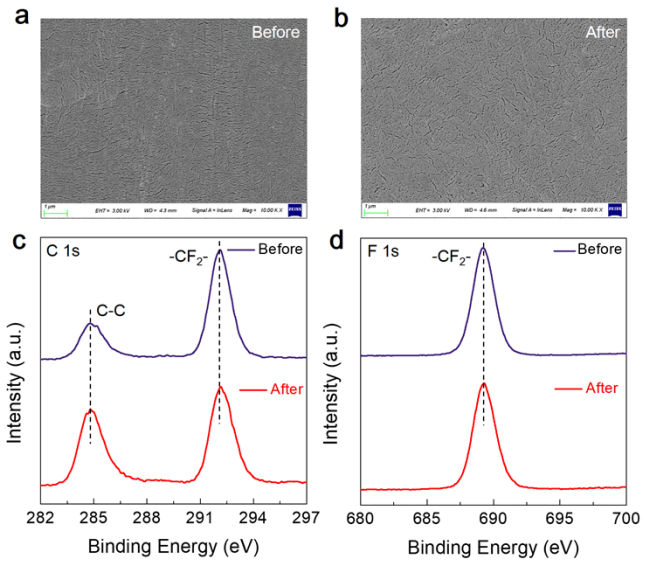

Figure S3. SEM (a, b) and XPS (c, d) characterization of PTFE stir bar before and after reaction.

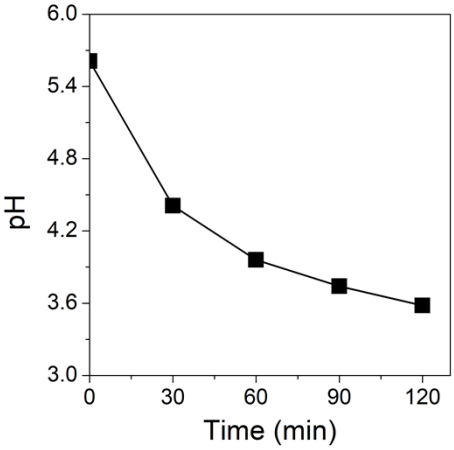

Figure S4. pH change of the solution in the PTFE stir bar + ultrasound system.

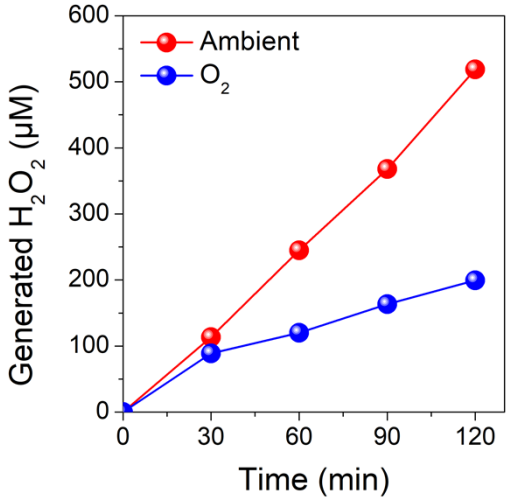

Figure S5. Effect of O_2 on the amount of H_2O_2 generation.

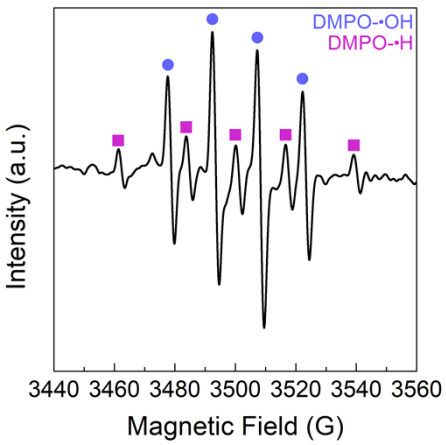

73

74 **Figure S6.** EPR signals for DMPO-•H in the PTFE stir bar + ultrasound system under

75 ambient atmospheric conditions.

76

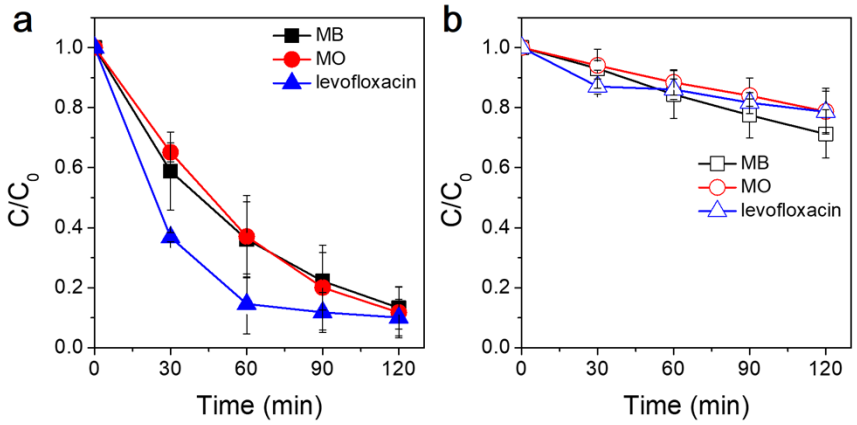

77

78 **Figure S7.** Pollutants degradation in the PTFE stir bar + ultrasound system (a) and pure

79 ultrasound system (b). $[MB]_0$=5 mg/L; $[MO]_0$=5 mg/L; $[levofloxacin]_0$=1 mg/L.

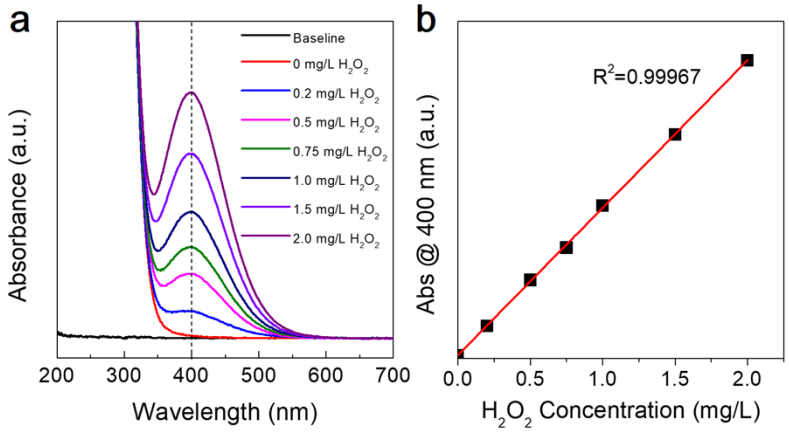

Figure S8. (a) Absorption spectrum of aqueous potassium titanium oxalate solution with different concentrations of H_2O_2. (b) The work curve of the concentration of H_2O_2 and the absorption.

Table S1. Comparison of H_2O_2 generation determined in the PTFE stir bar + ultrasound system and by piezocatalysis

Material	reaction solution	Atmosphere	Irradiation conditions	Reactor volume	H_2O_2 production rate ($\mu M\ h^{-1}$)	Ref.
C_3N_{5-x}-O	water	0.5 g L^{-1}	40 kHz, 300 W	20 mL	6.15	1
Au-$Bi_4Ti_3O_{12}$	water	2 g L^{-1}	40 kHz, 100 W	10 mL	8.1	2
$Cd_{0.5}Zn_{0.5}S$	water	2 g L^{-1}	40 kHz, 120 W	100 mL	11.0	3
V-$NaNbO_3$	water	~0.22 g L^{-1}	68 kHz, 192 W	45 mL	22.8	4
Bone-800	water	0.2 g L^{-1}	40 kHz, 150 W	50 mL	35.9	5
$Bi_4O_5I_2$	water	0.1 g L^{-1}	40 kHz, 240 W	100 mL	44.7	6
C-$KNbO_3$	water	2 g L^{-1}	-	25 mL	51.8	7
SnS_2/CNFs	water	0.8 g L^{-1}	40 kHz, 300 W	100 mL	~66.3	8
Fe/$BiVO_4$	water	0.5 g L^{-1}	40 kHz, 120 W	50 mL	~75	9
Au/$BiVO_4$	water	0.5 g L^{-1}	40 kHz, 120 W	50 mL	~86.1	10
$Ag_{(SA+C)}$-CN	water	0.02 g L^{-1}	40 kHz, 180 W	100 mL	117	11
$(Bi_{0.5}Na_{0.5})TiO_3$ cubes	water	0.1 g L^{-1}	40 kHz, -	100 mL	125	12
Bi_4TaO_8Cl	water	~0.33g L^{-1}	37 kHz, 110 W	30 mL	133	13
$RbBiNb_2O_7$/PTFE	water	~0.67 g L^{-1}	68 kHz, 240 W	30 mL	146.2	14
g-C_3N_4/PDI-g-C_3N_4	water	0.6 g L^{-1}	40 kHz, 200 W	50 mL	149.85	15
Ag/*t*-$BaTiO_3$	water	2.0 g L^{-1}	40 kHz, 110 W	200 mL	160.6	16
$BaTiO_3$-O_V	water	1 g L^{-1}	50 kHz, 100 W	50 mL	205	17
BiOCl	water	0.5 g L^{-1}	53 kHz, 150 W	100 mL	280	18
Hydroxyapatite	water	1.3 g L^{-1}	40 kHz, 300 W	25 mL	~304	19
PTFE stir bar	water	-	40 kHz, 300 W	50 mL	256.6	This work

Table S2. Comparison of H_2O_2 generation determined in the PTFE stir bar + ultrasound system and by photocatalysis

Material	reaction solution	Concentration of photocatalyst	Irradiation conditions	Reactor volume	H_2O_2 yield in 1 h ($\mu M\ h^{-1}$)	Ref.
C-N-g-C_3N_4	water	1.33 g L^{-1}	420 nm ≤ λ ≤ 700 nm 40 mW/cm^2	15 mL	1.0	20
g-C_3N_4 aerogels	water	1.7 g L^{-1}	>420 nm	30 mL	1.4	21
Cv-g-C_3N_4	water	1.0 g L^{-1}	300 W Xenon lamp >420 nm	100 mL	9	22
N-Cu_2O@CuO	water	1.5 g L^{-1}	300 W Xe lamp >420 nm	10 mL	12.6	23
g-C_3N_4/PDIx	water	1.67 g L^{-1}	>420 nm (intensity at 420–500 nm: 26.9 W/cm^2)	30 mL	35.2	24
NBCN-ZnPPc	water	0.5 g L^{-1}	Xe lamp 100 mW/cm^2, 800 nm >λ> 400 nm)	20 mL	57	25
CTF-BDDBN	water	0.6 g L^{-1}	300 W Xenon lamp >420 nm	50 mL	58.3	26
g-C_3N_4/PI	water	1.0 g L^{-1}	300 W Xe lamp >420 nm	50 mL	60	27
CN/rGO@BPQDs	water	1.0 g L^{-1}	300 W Xe lamp >420 nm	50 mL	60.6	28
g-C_3N_4-PWO	water	1.0 g L^{-1}	300 W Xe lamp >420 nm	100 mL	63	29
TiCOF-spn	Water	0.33 g L^{-1}	300 W Xenon lamp 420 nm ≤ λ ≤ 780 nm	120 mL	74.5	30
$Bi_4O_5Br_2$/g-C_3N_4	water	1.0 g L^{-1}	300 W Xe lamp >420 nm	50 mL	124	31
Au@MoS_2	water	1.0 g L^{-1}	300 W Xe lamp >420 nm	50 mL	132.0	32
Pd/APTMS/TiO_2	water	0.5 g L^{-1}	Xenon lamp solar simulator, 100 mW/cm^2	10 mL	150	33
HCOF	water	0.2 g L^{-1}	300 W Xenon lamp >420 nm	10 mL	153.3	34
Zn^{2+}/TiO_2	water	0.5 g L^{-1}	125 W Hg lamp	500 mL	220	35
Pt/TiO_2	water	0.05 g L^{-1}	500 W Hg lamp	20 mL	254.8	36
PTFE stir bar	water	-	40 kHz, 300 W	50 mL	256.6	This work

Supporting References

1. C. Fu, T. Wu, G. Sun, G. Yin, C. Wang, G. Ran, Q. Song, Dual-defect enhanced piezocatalytic performance of C_3N_5 for multifunctional applications, *Appl. Catal. B-Environ.* 2023, **323**, 122196.
2. R. Lei, X. Fu, N. Chen, Y. Chen, W. Feng, P. Liu, Cocatalyst engineering to weaken the charge screening effect over Au-$Bi_4Ti_3O_{12}$ for piezocatalytic pure water splitting, *Catal. Sci. Technol.* 2022, **12**, 7361-7368.
3. S. Lin, Q. Wang, H. Huang, Y. Zhang, Piezocatalytic and Photocatalytic Hydrogen Peroxide Evolution of Sulfide Solid Solution Nano-Branches from Pure Water and Air, *Small* 2022, **18**, 2200914.
4. Y. Li, L. Li, F. Liu, B. Wang, F. Gao, C. Liu, J. Fang, F. Huang, Z. Lin, M. Wang, Robust route to H_2O_2 and H_2 via intermediate water splitting enabled by capitalizing on minimum vanadium-doped piezocatalysts, *Nano Res.* 2022, **15**, 7986-7993.
5. Feixue Gao, Zhe Wang, Ming Fang1, Xiaoli Tan, Shao Hui Xu, Mao Liu, Guang Tao Fei, and Li De Zhang, Biological calcium phosphate nanorods for piezocatalytical extraction of U(VI) from water, *Nano Res.*, 2023, **16**, 12772-12780.
6. C. Wang, C. Hu, F. Chen, H. Li, Y. Zhang, T. Ma, H. Huang, Polar layered bismuth-rich oxyhalide piezoelectrics $Bi_4O_5X_2$ (X=Br, I): Efficient piezocatalytic pure water splitting and interlayer anion-dependent activity, *Adv. Funct. Mater.* 2023, **33**, 2301144.
7. J. He, F. Gao, H. Wang, F. Liu, J. Lin, B. Wang, C. Liu, F. Huang, Z. Lin, M. Wang, C-Doped $KNbO_3$ single crystals for enhanced piezocatalytic intermediate water splitting, *Environ. Sci.: Nano* 2022, **9**, 1952-1960.
8. W. Tian, J. Qiu, N. Li, D. Chen, Q. Xu, H. Li, J. He, J. Lu, Efficient piezocatalytic removal of BPA and Cr(VI) with SnS_2/CNFs membrane by harvesting vibration energy, *Nano Energy* 2021, **86**, 106036.
9. Y. Wei, Y. Zhang, J. Miao, W. Geng, M. Long, In-situ utilization of piezo-generated hydrogen peroxide for efficient p-chlorophenol degradation by Fe loading bismuth vanadate, *Appl. Surf. Sci.* 2021, **543**, 148791.
10. Wei, Y., Zhang, Y. W., Geng, W., Su, H. R., Long, M. C. Efficient bifunctional piezocatalysis of Au/$BiVO_4$ for simultaneous removal of 4-chlorophenol and Cr(VI) in water. *Appl. Catal. B-Environ.* 2019, **259**, 118084.
11. C. Hu, J. Hu, Z. Zhu, Y. Lu, S. Chu, T. Ma, Y. Zhang, H. Huang, Orthogonal charge transfer by precise positioning of silver single atoms and clusters on carbon nitride for efficient piezocatalytic pure water splitting, *Angew. Chem. Int. Ed.* 2022, **61**, e202212397.
12. D. Liu, X. Sun, L. Tan, J. Zhang, C.-C. Jin, F. Wang, High-performance piezocatalytic hydrogen evolution by $(Bi_{0.5}Na_{0.5})TiO_3$ cubes decorated with cocatalysts, *Ceram. Int.* 2023, **49**, 20343-20350.
13. M. Banoo, R. S. Roy, M. Bhakar, J. Kaur, A. Jaiswal, G. Sheet, U. K. Gautam, Bi_4TaO_8Cl as a new class of layered perovskite oxyhalide materials for piezopotential driven efficient seawater splitting, *Nano Lett.* 2022, **22**, 8867-8874.
14. Y. Ma, B. Wang, Y. Zhong, Z. Gao, H. Song, Y. Zeng, X. Wang, F. Huang, M.-R. Li, M. Wang, Bifunctional $RbBiNb_2O_7$/poly(tetrafluoroethylene) for high-efficiency

piezocatalytic hydrogen and hydrogen peroxide production from pure water, *Chem. Eng.* J. 2022, **446**, 136958.
15. R. Tang, D. Gong, Y. Zhou, Y. Deng, C. Feng, S. Xiong, Y. Huang, G. Peng, L. Li, Unique g-C_3N_4/PDI-g-C_3N_4 homojunction with synergistic piezo-photocatalytic effect for aquatic contaminant control and H_2O_2 generation under visible light, *Appl. Catal. B-Environ.* 2020, **303**, 120929.
16. J. X. Feng, Y. Fu, X. S. Liu, S. H. Tian, S. Y. Lan, Y. Xiong, Significant improvement and mechanism of ultrasonic inactivation to *Escherichia coil* with piezoelectric effect of hydrothermally synthesized *t*-$BaTiO_3$. *ACS Sustain. Chem. Eng.* 2018, **6**, 6032-6041.
17. P. Wang, X. Li, S. Fan, X. Chen, M. Qin, D. Long, M. O. Tadé, S. Liu, Impact of oxygen vacancy occupancy on piezo-catalytic activity of $BaTiO_3$ nanobelt, *Appl. Catal. B-Environ.* 2020, **279**, 119340.
18. Shao, D. K., Zhang, L., Sun, S. M., Wang, W. Z. Oxygen reduction reaction for generating H_2O_2 via piezo-catalytic process over bismuth oxychloride. *Chemsuschem* 2018, **11**, 527-531.
19. G. Yin, C. Fu, F. Zhang, T. Wu, S. Hao, C. Wang, Q. Song, Piezocatalytic degradation of organic dyes and production of H_2O_2 with hydroxyapatite, *J. Alloy. Compd.* 2023, **937**, 168382.
20. Y. Fu, C. a. Liu, M. Zhang, C. Zhu, H. Li, H. Wang, Y. Song, H. Huang, Y. Liu, Photocatalytic H_2O_2 and H_2 Generation from Living Chlorella vulgaris and Carbon Micro Particle Comodified g-C_3N_4, *Adv. Energy. Mater.* 2018, **8**, 1802525.
21. H. Ou, P. Yang, L. Lin, M. Anpo, X. Wang, Carbon Nitride Aerogels for the Photoredox Conversion of Water, *Angew. Chem. Int. Edit.* 2017, **129**, 11045-11050.
22. S. Li, G. Dong, R. Hailili, L. Yang, Y. Li, F. Wang, Y. Zeng, Effective photocatalytic H_2O_2 production under visible light irradiation at g-C_3N_4 modulated by carbon vacancies, *Appl. Catal. B-Environ.* 2016, **190**, 26-35.
23. W. Zhang, X. Chen, X. Zhao, M. Yin, L. Feng, Simultaneous nitrogen doping and Cu_2O oxidization by one-step plasma treatment toward nitrogen-doped Cu_2O@CuO heterostructure: an efficient photocatalyst for H_2O_2 evolution under visible light, *Appl. Surf. Sci.* 2020, **527**, 146908.
24. Y. Shiraishi, S. Kanazawa, Y. Kofuji, H. Sakamoto, S. Ichikawa, S. Tanaka, Sunlight-Driven Hydrogen Peroxide Production from Water and Molecular Oxygen by Metal-Free Photocatalysts, *Angew. Chem. Int. Edit.* 2014, **53**, 13454-13459.
25. Y.-X. Ye, J. Pan, F. Xie, L. Gong, S. Huang, Z. Ke, F. Zhu, J. Xu, Highly efficient photosynthesis of hydrogen peroxide in ambient conditions, *P. Natl. Acad. Sci. USA.* 2021, **118**, e2103964118.
26. L. Chen, L. Wang, Y. Wan, Y. Zhang, Z. Qi, X. Wu, Acetylene and diacetylene functionalized covalent triazine frameworks as metal-free photocatalysts for hydrogen peroxide production: a new two-electron water oxidation pathway, *Adv. Mater.* 2020, **32**, 1904433.
27. L. Yang, G. Dong, D. L. Jacobs, Y. Wang, L. Zang, Two-channel photocatalytic production of H_2O_2 over g-C_3N_4 nanosheets modified with perylene imides, *J. Catal.* 2017, **352**, 274-281.
28. J. Xiong, X. Li, J. Huang, X. Gao, Z. Chen, J. Liu, H. Li, B. Kang, W. Yao, CN/rGO@BPQDs high-low junctions with stretching spatial charge separation ability

for photocatalytic degradation and H_2O_2 production, *Appl. Catal. B-Environ.* 2020, **266**, 118602.
29. S. Zhao, X. Zhao, Polyoxometalates-derived metal oxides incorporated into graphitic carbon nitride framework for photocatalytic hydrogen peroxide production under visible light, *J. Catal.* 2018, **366**, 98-106.
30. W.-K. Han, H.-S. Lu, J.-X. Fu, X. Liu, X. Zhu, X. Yan, J. Zhang, Y. Jiang, H. Dong, Targeted construction of a three-dimensional metal covalent organic framework with spn topology for photocatalytic hydrogen peroxide production, *Chem. Eng. J.* 2022, **449**, 137802.
31. X. Zhao, Y. You, S. Huang, Y. Wu, Y. Ma, G. Zhang, Z:cheme photocatalytic production of hydrogen peroxide over $Bi_4O_5Br_2$/g-C_3N_4 heterostructure under visible light, *Appl. Catal. B-Environ.* 2020, **278**, 119251.
32. H. Song, L. Wei, C. Chen, C. Wen, Photocatalytic production of H_2O_2 and its in situ utilization over atomic-scale Au modified MoS_2 nanosheets, *J. Catal.* 2019, **376**, 198-208.
33. C. Chu, D. Huang, Q. Zhu, E. Stavitski, J. A. Spies, Z. Pan, J. Mao, H. L. Xin, C. A. Schmuttenmaer, Electronic tuning of metal nanoparticles for highly efficient photocatalytic hydrogen peroxide production, *ACS. Catal.* 2018, **9**, 626-631.
34. Q. Zhu, L. Shi, Z. Li, G. Li, Protonation of an Imine-linked Covalent Organic Framework for Efficient H_2O_2 Photosynthesis under Visible Light up to 700 nm, *Angew. Chem. Int. Edit.* 2024, e202408041.
35. V. Maurino, C. Minero, E. Pelizzetti, G. Mariella, A. Arbezzano and F. Rubertelli, Influence of Zn(II) adsorption on the photocatalytic activity and the production of H_2O_2 over irradiated TiO_2, *Res. Chem. Intermed.* 2007, **33**, 319-332.
36. L. Wang, S. Cao, K. Guo, Z. Wu, Z. Ma, Simultaneous hydrogen and peroxide production by photocatalytic water splitting, *Chin. J. Catal.* 2019, **40**, 470-475.